Global bifurcation approximation in controlling chaotic systems

Byoung-Cheon Lee, Bong-Gyun Kim and Bo-Hyeun Wang Information Technology Lab., LG Corporate Institute of Technology, 137-140, Seoul, Korea

January 26, 2011

Abstract

In our previous result[Lee et al., 1995], we demonstrated that return map control and adaptive tracking method can be used together to locate, stabilize, and track unstable periodic orbit(UPO) automatically. Our adaptive tracking method is based on the control bifurcation(CB) phenomenon which is another route to chaos generated by feedback control. Along the CB route, there are numerous driven periodic orbits(DPOs), and they can be good control targets if small system modification is allowed.

In this paper, we introduce a new control concept of global bifurcation approximation (GBA) which is quite different from the traditional local linear approximation (LLA). Based on this approach, we also demonstrate that chaotic attractor can be induced from periodic orbit. If feedback control is applied along the direction to chaos, small erratic fluctuations of periodic orbit is magnified and chaotic attractor is induced. One of a special feature of CB is the existence of irreversible orbit (IO) which is generated at the strong extreme of feedback control and has irreversible property. We show that IO induces a hysteresis phenomenon in CB, and discuss how to keep away from IO.

1 Introduction

The study of controlling chaos has been a hot issue since the historic study of OGY[Ott, Grebogie and Yorke, 1990]. They have shown that a lot of unstable periodic orbits(UPO) are embedded in a chaotic attractor and they can be stabilized by applying small time-dependent parametric perturbation. Basically, it is a feedback control method and is based on local linear approximation(LLA). They modeled a chaotic system as a linear system in the local vicinity of a fixed point. To start control, proper control conditions have to be determined through an extensive analysis of chaotic dynamics(reconstruction of chaotic attractor from a measured time-series, collecting data on a Poincare section map, locating the fixed point of an UPO, analyzing the stable and unstable manifold, and identifying its linear dynamics around the UPO). If a measured data occasionally gets into the local linear region, proper feedback control is applied and the UPO is stabilized. The requirement of an extensive prior analysis makes it difficult to apply OGY method for real fast systems.

A number of studies were followed to develop more efficient and easy methods applicable in real situations. Hunt[1991] used the occasional proportional feedback(OPF) method to control a fast diode resonator system. Roy et al.[1992, 1994] stabilized the output of a chaotic laser system using

OPF control. It is a simple experimental method, but there is no systematic way to get the proper control condition for a given control target. Pyragas's[1992] delayed continuous feedback method is an another simple approach. By delaying a time-series to certain delay time T and applying feedback perturbation continuously to itself, chaotic attractor is stabilized to UPO or fixed state. Return map control[Peng et al., 1991; Petrov et al., 1992; Petrov et al., 1994] is 1-d counterpart of OGY method. It is simpler than OGY because a return map of a time-series is considered rather than a Poincare map from reconstructed attractor. But considerable prior analysis is also required to start control.

Recently Lee et al. [1995] proposed that without extensive prior analysis, UPO can be located, stabilized and tracked automatically by applying return map control and adaptive tracking together. They also have shown the general existence of control bifurcation (CB) in feedback control which is another bifurcation phenomena as a function of control parameter of feedback control. The adaptive tracking method is based on the CB phenomenon. Along the CB route, there are numerous driven periodic orbits (DPOs) which are newly induced by feedback control. If small system modification is allowed, they can be good control targets.

In this paper, we will present how to manipulate chaotic systems using the CB phenomenon. In section 2, our previous results will be reviewed briefly using some updated data. In section 3, a new control concept of global bifurcation approximation(GBA) is introduced. As an extension of GBA, generation of chaos from periodic system is described. We show the existence of irreversible orbit and hysteresis phenomenon which limits the applicability of GBA. We discuss some considerations for real applications. Finally, conclusions are made in section 4.

2 Control bifurcation (CB) phenomenon and adaptive tracking method

2.1 Chua's circuit

For control study, we use Chua's circuit [Chua et al., 1986] as a model dynamical system. It is a simple electric circuit which shows a variety of dynamical behaviors from chaos to order [Shil'nikov, 1994]. Its simplified dynamical equations are

$$\dot{x} = A(y - x - f(x)),
\dot{y} = x - y + z,
\dot{z} = -By,$$
(1)

where $f(x) = bx + \frac{1}{2}(a-b)(|x+1| - |x-1|)$ is the piecewise-linear negative resistance, and A, B, a, and b are system parameters. For comparison, we will use a standard system parameter set(A = 8.3, B = 14.87, a = -1.27, and b = -0.68) which shows a double-scroll chaotic attractor. The default value of the Runge-Kutta integration time step h is set to 0.01.

2.2 Return map control

The return map control proposed by Petrov *et al.*[1991,1992,1994] is a simple feedback control scheme where a return map constructed from an available time-series is considered. For systems exhibiting low-dimensional chaos characterized effectively by one-dimensional maps, the OGY method can be reduced to a simple map-based algorithm. The simplified method is more convenient in real experimental applications.

Suppose a time-series X is available. We sample the local maximum states X_n of the time-series X and construct a return map of X_n vs. X_{n+1} . If the dynamics is chaotic, chaotic return map will appear. If there is a crossing between the chaotic return map and the diagonal line of $X_n = X_{n+1}$, it is the fixed point X_F of UPO and the slope around the UPO will be larger than 1 in negative sense. Analyzing the data points around the UPO, the stable and unstable manifold can be determined.

To stabilize the UPO, local linear approximation (LLA) in the local neighborhood of the UPO is made. Consider a control window of width X_W which denotes the local linear region. We model the chaotic return map as a linear system. The dynamics in the local vicinity of the fixed point X_F of UPO can be approximated by a linear equation of the following form

$$X_{n+1} = \lambda(X_n - X_F) + X_F, \tag{2}$$

where λ is the Floquet multiplier. The feedback perturbation required to stabilize the UPO is

$$\delta p = k(X_n - X_F),\tag{3}$$

where k is a proportionality constant and is given by

$$k = \frac{\lambda}{(\lambda - 1)\frac{\partial X_F}{\partial p}}. (4)$$

 $\partial X_F/\partial p$ represents the system response on parameter change. Once the orbit occasionally gets into the control window, proper feedback control δp is applied and the UPO is stabilized. To start control, the linear dynamic properties(λ and $\partial X_F/\partial p$) of the chaotic system have to be analyzed around the UPO.

As a standard control condition, we construct a return map from the time-series z and perturb the parameter A. So if it is not described specially, we are using the standard system condition and the standard control condition. The default width of control window X_W is set to 1.5 which is quite a wide control window in the point of traditional LLA.

2.3 Control bifurcation

Assume that the exact control condition to UPO, X_{F_0} and k_0 , was known and the system was stabilized to UPO. If the system response is studied as the control parameters, X_F and k, are varied around X_{F_0} and k_0 , a systematic response from chaotic attractor to periodic orbit is detected. Fig. 1 shows the variation of system dynamics under return map control when k is varied from zero to -0.23 for fixed $X_F = X_{F_0} = 4.2385$. When k = 0 which means no control, Chua's circuit shows double-scroll chaotic attractor and the slope $|\lambda|$ is larger than 1. For k = -0.15, the slope is decreased but still larger than 1 and the orbit shrinks to a period 2 orbit. If k is switched to -0.19, the slope become smaller than 1 and the orbit is slowly converged to UPO. For k = -0.23, the orbit is more fastly converged to UPO.

Using a bifurcation study as a function of control parameters, X_F and k, we identify it as an another bifurcation phenomenon induced by feedback control, and name it control bifurcation (CB). Typical CB diagrams are shown in Fig. 2. Fig. 2 (a) is the k-mode CB obtained by moving k from 0 to -0.4 for a given $X_F = X_{F_0}$ and fig. 2 (b) is the X_F -mode CB obtained by moving X_F from 4.2 to 4.6 for a given $k = k_0 = -0.2$. Although the origin of CB is different from the system bifurcation (SB) of the initial system, CB is qualitatively very similar to SB. The same period-doubling bifurcation appears in CB.

If we try return map control for other combinations of control input (time series used to construct a return map) and control output (parameter or state to which feedback perturbation is applied) including both parameter perturbation and state perturbation, we get similar results. Table 1 shows the k values of the first bifurcation point(B1) and the second bifurcation point(B2), and their ratios for all combinations of control input and control output. We can find B1 point for every combination, which represents that CB exists in every case. The sign of k values represent the direction to order and each combination has its own characteristic direction to order. The absolute values of k represent the sensitivity of the system response on the feedback perturbation. From eq. 4, we can see that larger k value represents smaller sensitivity of system response (control input) on the feedback perturbation (control output). The ratios of B1/B2 are consistent in every case, which represents that CB has common scaling property.

The data corresponding to control input y or control output y show exception. In these cases, identification of B2 point is very difficult and the scaling is not consistent. It can be understood from the fact that the two scrolls of Chua's circuit coexist in the same region for the time series y. If two UPOs are in the same region and a global feedback control is made, one UPO can effect the other UPO through feedback control. So stabilization of one UPO becomes difficult.

Table 1: The k values of B1 and B2, and their ratios for all combinations of control input and control output.

	In	x	37	Z	
Out		$X_{F_0} = 2.7771$	$X_{F_0} = 0.5473$	$X_{F_0} = 4.2385$	
	B1	+0.937	-3.170	$\frac{11_{F_0}}{-0.454}$	
X	B2	+0.725	0.110	-0.345	
Λ	ratio	1.292		1.316	
	B1	+(*)	-8.100	-0.805	
••	B2	T(*)	-6.100	-0.803	
У					
	ratio				
	B1	+1.410	-6.540	-0.833	
${f z}$	B2	+1.080		-0.640	
	ratio	1.306		1.302	
	B1	-0.364	-4.000	-0.184	
A	B2	-0.279		-0.140	
	ratio	1.305		1.314	
	B1	+0.384	+5.600	+0.165	
В	B2	+0.305		+0.126	
	ratio	1.259		1.310	
	B1	+0.099	+0.490	+0.053	
a	B2	+0.076		+0.040	
	ratio	1.301		1.332	
	B1	+0.326	+1.470	+0.214	
b	B2	+0.260		+0.165	
	ratio	1.254		1.297	

^{(*) +1.563} with d = 1.8.

To get more systematic information about the CB structure of return map control, we search for the distribution of bifurcation points in the control parameter space (X_F, k) . Fig. 3 (a) shows the distribution of bifurcation points around UPO. A unified and continuous CB structure seems to exist in the control parameter space. Fig. 3 (b) shows the 3-d view of the mean of feedback perturbations at the bifurcation points. Note that the only UPO is $X_F = X_{F_0}$ for $k < k_{b_1} = -0.184$ and the feedback perturbations have zero-mean only at UPO.

2.4 Adaptive tracking method

The CB phenomenon suggests a possibility of automatic control to UPO. For each CB, there are two directions, one to order and the other to chaos. The direction to order can be determined simply by observing the change of dynamical range as some small test feedback is applied. If the dynamical range shrinks along a direction, it is the direction to order.

If we consider the k-mode CB, UPO can be traced by adjusting k value along the direction to order until the running deviation of measured data is reduced to zero. On the other hand, if we consider the X_F -mode CB, the location of UPO can be traced automatically by adjusting X_F to the running average of measured data. When UPO is stabilized, the feedback perturbation will be minimized to small zero-mean perturbation.

Based on this idea, we developed the following simple adaptive tracking equations.

$$X_F(n+1) = X_F(n) + \alpha(X^* - X_F(n)),$$
 (5)

$$k(n+1) = k(n) + sgn(k(n))\beta\delta^*.$$
(6)

 X^* is the running average and δ^* is the running deviation of measured data. α and β are some stiffness constants of the adjustment and sgn(k(n)) is the predetermined direction to order.

The overall control flow including both return map control and adaptive tracking is shown in fig. 4. The adaptive tracking module analyzes the system response under the return map control, and calculates running average X^* and running deviation δ^* . Using the tracking equations (5) and (6), the control parameters, X_F and k, are updated at each step of return map until the perturbation converges to small zero-mean value.

2.5 Locating, stabilizing and tracking UPO using adaptive tracking

Applying return map control and adaptive tracking together, UPO can be automatically located and stabilized without knowing the exact control condition. Fig. 5 shows an example of automatic searching and stabilization of UPO. We try a rather global control setting $X_W = 1.5$. Starting from an approximate control condition of $X_F = 4.2$ and k = -0.1, we apply the adaptive tracking. Note that the fixed point X_F is adjusted continually and the control signals (small horizontal bars) converge rapidly to zero. The experimentally tracked exact location of the fixed point and its control condition are $X_{F_0} = 4.2385$ and $k_0 = -0.2$.

Fig. 6 shows the results of tracking UPO using our adaptive tracking method when the system parameter A moves slowly. Fig. 6 (a) represents the tracking of the period 1 UPO(UPO₁) when A moves slowly from 7.5 to 9.0. As A increases, the system goes to more chaotic regime and the control to UPO₁ becomes unstable. The adaptive tracking module given by eqs. (5) and (6) detects the change of the system responses under the parameter change and updates the control conditions, X_F and k, until the feedback perturbations converge to small zero-mean value. Fig. 6 (b) represents the tracking of the period 3 UPO(UPO₃) when A moves slowly from 8.1 to 8.5.

We target the topmost fixed point among the 3 possible fixed points and select a narrow control window of $X_W = 0.2$.

2.6 Control to DPO

The CB diagrams suggest us that there are numerous periodic orbits around UPO. All the periodic orbits except UPO are some kind of *driven periodic orbits*(DPOs) which are generated artificially by driving the chaotic system in a direction with feedback control. To stabilize UPO, only small zero-mean feedback perturbation is required. On the other hand, to stabilize DPOs, we should drive the system with quite a lot non-zero-mean feedback perturbations.

Fig. 7 shows the distribution of UPO, DPOs, and the original chaotic attractor. (a) is the original chaotic attractor without any control. (b) is the stabilized UPO with $X_F = X_{F_0} = 4.2385$ and k = -0.2. Note that it is embedded in the original chaotic attractor. (c) is a period 2 DPO(DPO₂) generated with $X_F = X_{F_0}$ and k = -0.17, and (d) is another period 2 DPO(DPO₂) generated with $X_F = 4.27$ and k = -0.2. (e) is a period 1 DPO(DPO₁) generated with $X_F = 4.15$ and k = -0.2. These DPOs are not embedded in the original chaotic attractor and they are generated artificially by feedback control.

If user requires slightly different periodic orbits rather than UPO and small system modification is allowed, these abundant DPOs can be good control targets.

3 Global bifurcation approximation

Our control methodology described above is quite different from the traditional feedback control methods based on the local linear approximation(LLA). The basic idea of LLA is that the chaotic dynamics of nonlinear system can be approximated as a linear dynamics in the local neighborhood of UPO. To start control, one has to analyze the system dynamics in the local linear region around UPO and reconstruct the linear dynamics. If a measured state is occasionally come into the local linear region, proper feedback perturbation proportional to the difference between the measured state and the targeted fixed point is applied to stabilize UPO.

Compared with LLA, we consider the CB phenomenon in a relatively wider control window around UPO. UPO is located along the CB route and it can be stabilized automatically using adaptive tracking. This approach can be referred as global bifurcation approximation (GBA). In GBA, the chaotic system is approximated as a bifurcation dynamics over a global control window. The advantage of GBA is that it does not require extensive prior analysis to reconstruct a linear dynamics. To start control, we don't need to wait until the system occasionally visits the local linear region. Control can be started immediately. Tracking is also very easy for fastly changing system because GBA considers wider control window while LLA considers only local linear region.

CB seems to be a universal phenomenon, so GBA is applicable to any chaotic systems or feedback control methods. Control target is not restricted only to UPO, but abundant DPOs and the whole dynamical ranges are also available using GBA. In this section, we will describe how GBA is extended to other control jobs such as generating chaos from periodic orbits. We will discuss some limitations of GBA and considerations for real application.

Table 2: An example of generation of chaos from a periodic system. k values of the first bifurcation point(B1) from the period 1 orbit to the period 2 orbit are shown for all combinations of control input and control output.

In	X	У	\mathbf{z}
Out	$X_{F_0} = 2.8108$	$X_{F_0} = 0.5621$	$X_{F_0} = 4.3627$
X	-0.078	+0.230	+0.040
y	?	+1.260	?
${f z}$	-0.138	+0.380	+0.078
A	+0.032	+4.800	+0.018
В	-0.033	-3.300	-0.015
a	-0.009	-0.033	-0.005
b	-0.031	-0.490	-0.023

3.1 Feedback generation of chaos from periodic system

The same principle of feedback control based on GBA can be used to generate chaotic attractor from periodic orbit. Firstly, we take an eye on the fact that although it is a periodic system, small fluctuation can be accompanied due to small mismatch of sampling time or measurement errors. Fig. 8 (a) shows a close-up view of return map for a periodic system of A=7.7. It shows small fluctuations around the period 1 orbit. Secondly, we consider the fact that there are two directions along the CB route, one to order and the other to chaos. If feedback control is applied along the direction to order, chaotic attractor is shrunk to periodic orbit. But if feedback control is applied to opposite direction(direction to chaos), chaotic attractor will expand to more chaotic regime. What happens if feedback control is applied for periodic systems along the direction to chaos?

In this control condition, the direction to chaos is positive. Fig. 8 (b) is the result of applying feedback with k = 0.018. A loop of fluctuation tends to separate to two loops. Fig. 8 (c) is a bifurcation diagram when k is varied from 0 to 0.2. Another CB is obtained. It seems to be a very special feature because amplifying small erratic fluctuations with feedback control along the direction to chaos, we get a chaotic attractor which has qualitatively similar property to the original chaotic attractor. It can be said that using feedback control, generation of chaos from periodic system is also possible under the same theoretical basis.

The generation of chaos from periodic system is different from changing the system itself. It is generated by just amplifying small fluctuations by feedback control. So it can be readily applicable to any real situation for which the system can not be modified. For example, in the case of mixing fluid, chaotic dynamics is more preferable than periodic motion. Without changing the system itself, chaotic motion can be induced from periodic system just by feedback control.

To compare this results with the original CB, we measure the k values of the first bifurcation points(B1) which represent the escaping points from period 1 orbit to period 2 orbit. Table 2 shows the k values of B1 points for every combinations of control input and control output. Note that compared with the values of table 1, the signs of each k value are opposite and the absolute values have similar scaling property. The scaling of values corresponding to control input y or control output y are not consistent. It is because the two scrolls coexist in the same region for the time-series y.

Table 3: Scaling property in UPO and IO. k values of the first bifurcation point(B1) and the switching point(SP) from UPO to IO and their ratios are shown for all combinations of control input and control output.

In		X			Z	
Out	B1	SP	ratio	B1	SP	ratio
X	+0.937	+2.300	2.455	-0.454	-0.950	2.093
У	+(*)			-0.805		
${f z}$	+1.410	+3.200	2.270	-0.833	-1.760	2.113
A	-0.364	-0.890	2.445	-0.184	-0.380	2.065
В	+0.384	+0.970	2.526	+0.165	+0.348	2.110
a	+0.099	+0.236	2.384	+0.053	+0.110	2.076
<u>b</u>	+0.326	+0.750	2.301	+0.214	+0.440	2.056

(*) +1.563 with d = 1.8.

3.2 Irreversible orbit and hysteresis phenomenon in control bifurcation

The CB diagram of fig. 2 (a) shows that UPO can be stabilized over a wide range of k value, so automatic control to UPO is very reliable. But a different orbit appears at the strong extreme of feedback control of k < -0.38. This orbit has irreversible property. Once the system is switched to this irreversible orbit(IO) along the CB route, it shows different track in the other direction.

Fig. 9 shows the close-up view of return map when the system switches from UPO to IO along the CB route. (a) is the case of k = -0.2 which shows a closed fluctuation loop with zero-mean perturbation. (b) is the case of k = -0.3 which shows an enlarged fluctuation loop also with zero-mean perturbation. (c) is the case of k = -0.38 which shows a slightly shifted loop with non-zero-mean perturbation. If k < -0.38, the system switches to IO.

The irreversible property of IO causes hysteresis phenomenon in CB. Fig. 10 shows some examples. Fig. 10 (a) is a k-mode CB for A=8.5. As k moves from 0 to -0.6 along the direction to order, UPO is stabilized through a reverse bifurcation and then switched to IO for k<-0.5. But, as k moves from -0.6 to 0 along the direction to chaos, IO is maintained to k<-0.3 and then switched back to UPO. In this case, UPO is stabilized only in narrow range of k values. Fig. 10 (b) is a k-mode CB for A=9.0. In this case, UPO can be stabilized in the direction to order, but it can not be stabilized in opposite direction. So in this case, automatic control to UPO using adaptive tracking is rather difficult.

To study the scaling property of UPO and IO, we investigate the B1 point from UPO to period 2 orbit and switching point(SP) from UPO to IO along the direction to order. Table 3 shows the k values of B1, SP and their ratios for every combinations of control input and control output. The ratios of two values also show consistent scaling property. It can be said that UPO can be stabilized to the same extent for every combinations of control input and control output.

3.3 Considerations for real application

The existence of hysteresis phenomenon in CB suggests that we have to use our linear tracking equations, (5) and (6), carefully. If control parameter is adjusted over the range of UPO, the system will be switched to IO and it will be hard to come back to UPO. For automatic control to be used

successfully, we have to manage hysteresis phenomenon properly to overcome the switching to IO.

Then, how can we keep the system away from IO? Firstly, we have to start control slowly from small test control. Using the result of test control, we determine the direction to order and the system response on feedback perturbation. The stiffness constants of eq. (5), (6) can be adjusted continually depending on the system response on feedback perturbation. Secondly, we have to use the information of CB phenomenon and IO. All the control procedure have to be seriously analyzed to characterize the CB route, IO, and hysteresis phenomenon. If systematic control bifurcation is not detected or some irreversible orbits are encountered, the adaptive tracking procedure has to be stopped.

If we try to control a nonlinear dynamical system, we will use a hierarchical combination of the chaos control technique and other traditional control techniques. In this case, the chaos control technique will serve as a basic control algorithm to deal with the nonlinear property. Other control techniques such as fuzzy or neural net can organize the proper control operations depending on the information of CB and IO.

Although GBA has some drawbacks such as IO, it suggests a new methodology for the control of chaotic systems. It is considered that GBA is generally applicable to chaotic systems which show CB phenomenon. For low dimensional chaotic systems, CB is generally observed and it seems to be a universal phenomenon. But in the case of higher dimensional systems, much further research has to be followed.

4 Conclusions

Compared with the traditional local linear approximation, we introduced a new control concept of global bifurcation approximation based on the control bifurcation phenomenon. Using GBA, control to UPO is very easy and efficient. We can start control immediately without extensive prior analysis. There are numerous DPOs around UPO and they can be good control targets if we need slightly different periodic orbits rather than UPO and small system modification is allowed. Using the same methodology, chaotic attractors can be generated from periodic orbit by amplifying small erratic fluctuations using feedback control along the direction to chaos. This technology is very effective when system modification is rather difficult. At the strong extreme of feedback control along the CB route, there is irreversible orbit(IO) which has irreversible property in CB. It causes hysteresis phenomenon in CB and limits the applicability of automatic control based on GBA. More hierarchical approach is required to manage the hysteresis phenomenon and keep the system away from IO.

References

Chua, L. O., Komuro, M. & Matsumoto, T. [1986] "The double scroll family", *IEEE Trans. Circuits and Systems* CAS-33, 1072–1118.

Hunt, E. R. [1991] "Stabilizing high-period orbits in a chaotic system: The diode resonator", *Phys. Rev. Lett.* **67**, 1953–1955.

Lee, B. C., Lee, K. H. & Wang, B. H. [1995] "Control bifurcation structure of return map control in Chua's circuit", (Presented at NLDC-95, Pohang, Korea and will appear in Int. J. Bifurcation and Chaos)

Ott, E., Grebogie, C. & Yorke, J. A. [1990] "Controlling chaos", *Phys. Rev. Lett.* **64**, 1196–1199. Peng, B., Petrov, V. & Showalter, K. [1991] "Controlling chemical chaos", *J. Chem. Phys.* **96**, 7506–7513.

Petrov, V., Peng, B. & Showalter, K. [1992] "A map-based algorithm for controlling low-dimensional chaos", J. Phys. Chem. **95**, 4957–4959.

Petrov, V., Crowley, M. F. & Showalter, K. [1994] "An adaptive control algorithm for tracking unstable periodic orbits", *Int. J. Bifurcation Chaos*, 4, 1311–1317.

Pyragas, K. [1992] "Continuous control of chaos by self-controlling feedback", *Phys. Lett.*, **A170**, 421–428.

Roy, R., Murphy, T. W., Maier, T. D., Gills, Z. & Hunt, E. R. [1992] "Dynamical control of a chaotic laser: Experimental stabilization of a globally coupled system", *Phys. Rev. Lett.*, **68**, 1259–1262.

Roy, R., Gills, Z. & Thornburg, S. [1994] "Controlling chaotic lasers", Optics & Photonics News, May, 8–14.

Shil'nikov, L. P. [1994] "Chua's circuit: Rigorous results and future problems", *Int. J. Bifurcation Chaos*, 4, 489–519.

Figure Captions

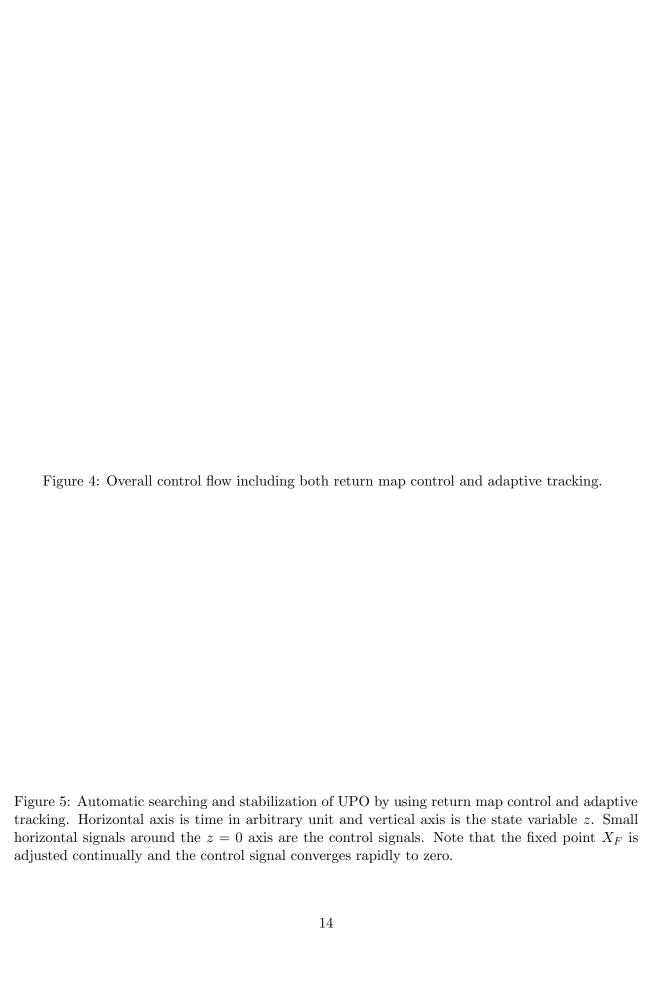
Figure 1: Return map showing the control dynamics when k is varied from 0 to -0.23 for $X_F = X_{F_0} = 4.2385$. (a) k = 0, double-scroll attractor with no control, (b) k = -0.15, converge to period 2 orbit, (c) k = -0.19, control to UPO with slow convergence, (d) k = -0.23, control to UPO with slow convergence.

(b)

Figure 2: Typical control bifurcation diagrams. (a) k-mode CB with $X_F=X_{F_0}=4.2385$, (b) X_F -mode CB with $k=k_0=-0.2$.

(b)

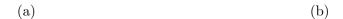
Figure 3: Control bifurcation structure of return map control in (X_F, k) space. (a) Distribution of bifurcation points in (X_F, k) space, (b) 3D view of the mean of the feedback perturbation at the bifurcation points.



(b)

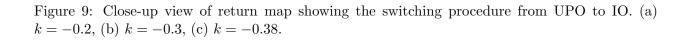
Figure 6: Tracking UPO using adaptive tracking method. Circled solid line represents the tracked UPO. (a) Tracking the period 1 UPO(UPO₁) when A moves from 7.5 to 9.0, (b) Tracking the period 3 UPO(UPO₃) when A moves from 8.1 to 8.5.

Figure 7: Return map showing control to UPO and DPOs compared with the uncontrolled chaotic attractor. (a) Uncontrolled chaotic attractor, (b) control to UPO with $X_F = X_{F_0} = 4.2385$ and $k = k_0 = -0.2$, (c) control to period 2 DPO with $X_F = X_{F_0}$ and k = -0.17, (d) control to period 2 DPO with $X_F = 4.27$ and $k = k_0$, (e) control to period 1 DPO with $X_F = 4.15$ and $k = k_0$.



(c)

Figure 8: Generation of chaos from periodic system of A=7.7 using feedback control along the direction to chaos. (a) Close-up view of return map of uncontrolled periodic orbit, (b) that of separating loop with k=0.018, (c) bifurcation diagram which shows the generation of chaos from periodic system.



(b)

Figure 10: Hysteresis diagrams in CB. Control from the time-series z to the parameter A. (a) A=8.5, (b) A=8.5.